Title

Enhanced survival and engraftment of transplanted stem cells using growth factor sequestering hydrogels

Authors

Jha, Amit K
Tharp, Kevin M
Ye, Jianqin
et al.

Publication Date

2015-04-01

DOI

10.1016/j.biomaterials.2014.12.043

Peer reviewed

HHS Public Access

Author manuscript

Biomaterials. Author manuscript; available in PMC 2016 April 01.

Published in final edited form as:

Biomaterials. 2015 April ; 47: 1–12. doi:10.1016/j.biomaterials.2014.12.043.

Enhanced Survival and Engraftment of Transplanted Stem Cells using Growth Factor Sequestering Hydrogels

Amit K. Jha[1,2], **Kevin M. Tharp**[3], **Jianqin Ye**[4], **Jorge L. Santiago-Ortiz**[5], **Wesley M. Jackson**[1], **Andreas Stahl**[3], **David V. Schaffer**[1,5], **Yerem Yeghiazarians**[4,6,7], and **Kevin E. Healy**[1,2,*]

[1]Department of Bioengineering, University of California, Berkeley, CA 94720, USA

[2]Department of Material Science and Engineering, University of California, Berkeley, CA 94720, USA

[3]Department of Nutritional Science and Toxicology, University of California, Berkeley, CA 94720, USA

[4]Department of Medicine, University of California, San Francisco, CA 94143, USA

[5]Department of Chemical and Biomolecular Engineering, University of California, Berkeley, CA 94720, USA

[6]Eli and Edythe Broad Center of Regeneration Medicine and Stem Cell Research, University of California, San Francisco, CA 94143, USA

[7]Cardiovascular Research Institute, University of California, San Francisco, CA 94143, USA

Abstract

We have generated a bioinspired tunable system of hyaluronic acid (HyA)-based hydrogels for Matrix-Assisted Cell Transplantation (MACT). With this material, we have independently evaluated matrix parameters such as adhesion peptide density, mechanical properties, and growth factor sequestering capacity, to engineer an environment that imbues donor cells with a milieu that promotes survival and engraftment with host tissues after transplantation. Using a versatile population of Sca-1^+/$CD45^-$ cardiac progenitor cells (CPCs), we demonstrated that the addition of heparin in the HyA hydrogels was necessary to coordinate the presentation of TGFβ1 and to support the trophic functions of the CPCs via endothelial cell differentiation and vascular like tubular network formation. Presentation of exogenous TGFβ1 by binding with heparin improved differentiated CPC function by sequestering additional endogenously-produced angiogenic factors. Finally, we demonstrated that TGFβ1 and heparin-containing HyA hydrogels can promote CPC survival when implanted subcutaneously into murine hind-limbs and encouraged their participation in the ensuing neovascular response, including blood vessels that had anastomosed with the host's blood vessels.

*To whom correspondence should be addressed: Kevin E. Healy, University of California Berkeley, 370 Hearst Memorial Mining Building, MC1760, Berkeley, CA 94720, Phone: 510-643-3559, kehealy@berkeley.edu.

1. Introduction

Over the past decade, stem cell transplantation therapy has started to fulfill its long held promise as a means of promoting functional regeneration of tissues that have been damaged by injury and disease. As new cell therapies have translated into clinical studies, modest results have been reported for regeneration in several tissue types, including cardiac[1, 2], skeletal muscle[3], and liver[4]. These studies pointed out several technological challenges regarding relevant cell transplantation parameters that must be optimized before these treatment options become widely available. One pressing problem is that immediately after transplantation into damaged tissue, donor cells encounter a harsh environment with substantial death-promoting stimuli (e.g., hypoxia, reactive oxygen species, etc.), and the vast majority (>90%) of donor cells are lost to necrosis and/or apoptosis within hours to days after transplantation [5, 6]. Based on the poor cell survival rate after transplantation, there has been limited evidence that the donor cells can engraft and functionally integrate with the damaged tissue to participate directly to regeneration processes [7–9]. Instead, recent evidence indicates that paracrine signaling of the transplanted cells is the major contributor to any significant tissue regeneration observed [10–12].

One strategy for improving the survival of transplanted stem or progenitor cells, termed Matrix-Assisted Cell Transplantation (**MACT**), is to engineer a materials-based environment that promotes pro-survival paracrine signaling immediately after transplantation, and subsequently stimulates mechanisms of cell engraftment with the host tissues [13–19]. Matrigel™ was initially proposed as a material for MACT, but heterogeneous batch-to-batch material composition, quality control and biological sourcing issues, and the inability to engineer design changes have substantially impeded its clinical translation. Therefore, recent advances in this field have focused on transplanting cells with other natural or synthetic matrices [20–25]. Most work has focused on naturally occurring biopolymers such as collagen, alginate, fibrin, chitosan, and hyaluronic acid (HyA), with alginate and fibrin modestly attenuating the negative remodeling process. Ideally a material for MACT would exploit not only the pro-survival potential of naturally occurring biopolymers, but also allow for a wide design space to modulate parameters that are relevant in a pro-healing native extracellular matrix, including the ability to harness endogenously synthesized growth factors by sequestering them in the matrix.

To overcome the limitations that are currently associated with MACT, we have developed hyaluronic acid (**HyA**) -based hydrogels that were generated using a tunable method of synthesis. HyA was selected as the primary component of this structural matrix since it is biocompatible, biodegradable, non-immunogenic, and plays a critical role in fostering tissue development and repair [26]. Our method of synthesis enabled *independent* control over the hydrogel mechanical properties and biological features, including: (1) the density of peptide sequences for cell attachment via binding to integrin receptors; (2) matrix modulus; (3) the cell-mediated degradation kinetics by selective the MMPs[21]; and, (4) sequestration of exogenously added or endogenously synthesized growth factors via heparin conjugated within the hydrogel. Previously reported materials for MACT have not simultaneously

explored the effect of all these matrix parameters on transplanted cell survival and engraftment.

Regarding the use of heparin, it is well known soluble growth factors have their effect on cells for limited time due to their poor stability, soluble presentation, and short half-life in *vivo*. A number of groups have demonstrated that heparin can sequester and release exogenously added growth factors that ultimately improve wound healing and tissue regeneration [27–32]. Therefore, thiolated heparin macromers were incorporated into HyA based hydrogels for solid-phase presentation and prolonged retention of growth factors that were either added exogenously or endogenously produced by the entrained cells.

Using this easily tunable hydrogel system, the objective our study was to demonstrate how a suitable material for MACT can support donor cell survival during transplantation and encourage donor cell integration with the host tissue. In this study, we focused on murine cardiac progenitor cells (**CPCs**), a pluripotent population of GFP^+ $Sca\text{-}1^+/CD45^-$ cells that contribute to cardiac regeneration, at least in part by undergoing neovascular differentiation that is characteristic of endothelial cells [10, 33]. With this versatile cell type, we examined how the biochemical and mechanical parameters of the HyA hydrogels influenced: (1) CPC survival, proliferation, and differentiation *in vitro*; and, (2) CPC survival and functional integration via neovascularization *in vivo*.

2. Materials & Methods

2.1 Materials

Hyaluronic acid (HyA, sodium salt, 1.0 MDa and 500 kDa) was generously donated by Lifecore Biomedical (Chaska, MN). Adipic dihydrazide (ADH), 1-ethyl-3-[3-(dimethylamino)propyl] carbodiimide (EDC), sodium hydroxide (NaOH), hydrochloric acid (HCl) and 1-hydroxybenzotriazole (HOBt) were purchased from Aldrich (Milwaukee, WI). Dimethyl sulfoxide (DMSO), N-Acryloxysuccinimide (NAS), acetone, ethanol were obtained from Fisher Scientific (Waltham, MA). Paraformaldehyde (16% in H_2O) was obtained from Electron Microscopy Sciences (Hartfield, PA). Calcein was purchased from BD Biosciences (Pasadena, CA). The MMP-degradable crosslinker peptide (CQPQGLAKC) and the 15 aminoacid adhesion peptide (CGGNGEPRGDTYRAY), bsp-RGD(15), were synthesized by American Peptide (Sunnyvale, CA). Dialysis membranes (10000 MWCO, SpectraPor Biotech CE) were purchased from Spectrum Laboratories (Rancho Dominguez, CA). All chemicals were used as received. All cell culture reagents were purchased from Invitrogen (Carlsbad, CA). 1× Dulbecco's phosphate buffered saline (DPBS) was purchased from Invitrogen.

2.2. Synthesis of AcHyA hydrogel components

Functionalization of HyA with acrylate groups using a two-step synthesis method and functionalization of heparin with a thiol group were performed as follows (Supplementary Fig. S1):

1. *Acrylation of HyA*: A HyA derivative carrying hydrazide groups (HyA-ADH) was synthesized using a previously reported method[34]. Specifically, 30 molar excess

of ADH was added to HyA in deionized (DI) water (100 ml, 3 mg/ml). Solution pH was adjusted to 6.8 using 0.1M NaOH and 0.1M HCl. EDC (3 mmol) and HOBt (3 mmol) were dissolved separately in DMSO/water (1/1 volume ratio, 3 ml) and added to the HyA solution sequentially. The solution was allowed to react for 24 hours, and the pH was maintained at 6.8 for at least the first 6 h. After 24 hrs, the solution pH was adjusted to 7.0 and exhaustively dialyzed against DI water. Then, NaCl was added to produce a 5% (w/v) solution, and HyA-ADH was precipitated in 100% ethanol. The precipitate was redissolved in H_2O and dialyzed again to remove the salt. Subsequently, NAS (700 mg) was reacted to the HyA-ADH solution (300mg, 100 mL DI water) to generate acrylate groups on the HyA) [22]. The product was then lyophilized for 3 days to obtain acrylated HyA (AcHyA). Using a previously described analysis [35], proton (^1H) NMR confirmed that ~28% of the available carboxyl groups were conjugated with acrylate groups on the final acrylated HyA product (AcHyA; Supplementary Fig. S2).

2. *Synthesis of Thiolated Heparin (heparin-SH):* Heparin-SH synthesis was adapted from a previous report [36]. Heparin (50mg) was dissolved in DI water at a concentration of 5 mg/mL and reacted with an excess amount of cystamine in the presence of EDC and HOBt at pH 6.8 for 5 h at room temperature. Next, the reaction solution was exhaustively dialyzed using a dialysis cassette to remove all small molecules not attached to heparin, and then the reaction product was lyophilized. After that, a 10-fold molar (moles per COOH of heparin) excess of tris (2-carboxyethyl) phosphine (TCEP) was added to reduce the oxidized disulfide groups in order to reduce any disulfide bonds that had formed between thiol groups. This solution was allowed to react for 3 h at pH 7.5 and then adjusted to pH 5.0 by the addition of 1.0 N HCl. The acidified solution was dialyzed against dilute HCl (pH 5.0) containing 100 mM NaCl, followed by dialysis against dilute HCl at pH 5.0. Then heparin-SH was lyophilized for 3 days, and the percentage of conjugation of thiol groups on the final product (heparin-SH) was determined by colorimetric Ellman assay.

2.3. Synthesis of HyA hydrogels

Prior to making HyA hydrogels, AcHyA-RGD derivative was synthesized by reacting CGGNGEPRGDTYRAY (**bsp- RGD(15)**) (10mg) with AcHyA solution (25mg, 10mL DI water) at room temperature. AcHyA (13.3 mg/mL), AcHyA-RGD (20 mg/mL), and heparin-SH (0.013 mg/mL) were dissolved in 0.3 mL of triethanolamine-buffer (TEOA; 0.3 M, pH 8), and incubated for 15 minutes at 37 °C. HyA hydrogels were generated by *in situ* crosslinking of the HyA precursors with the MMP-13-cleavable peptide sequence CQPQGLAKC (50μL TEOA buffer) [21, 37]. Viscoelastic properties of the hydrogel were determined by an oscillatory rheometer (MCR 302 Modular Compact Rheometer; **Anton Paar**, Ashland, VA) with a parallel plate geometry (25mm diameter) under 10% constant strain and frequency ranging from 0.1 Hz to 10 Hz.

2.4. Incorporation of TGF-β1 and Measurement of Retention Kinetics

Hydrogel macromers of AcHyA (13.3 mg/mL), AcHyA-RGD (20 mg/mL), and heparin-SH (0.013 mg/mL) were dissolved at various ratios (Supplementary table S1) in 0.3 mL of triethanolamine-buffer (TEOA; 0.3 M, pH 8) and incubated for 15 minutes at 37 °C. Then, TGFβ1 (350 ng, Cell Signaling Technology, Danvers, MA) was mixed in the solution of HyA derivatives and incubated for another 15 min at 37°C. To determine the release kinetics, TGFβ1 containing HyA hydrogels were transferred to cell culture inserts (Millipore Corporation, Billerica, MN) and TGFβ1 was allowed to release into 400 μL of cell culture media per well. At predetermined time points over the course of 3 weeks, the supernatant was withdrawn and fresh media was replenished, and the mass of TGFβ1 in each supernatant was determined with sandwich ELISA kits (RayBiotech, Inc, Norcross GA) (Supplementary Fig 5a, b). Retention of TGFβ1 was calculated by the subtraction of released TGFβ1 from the calculated initial loading amount of TGFβ1 (Supplementary Fig 5a). Similarly, retention kinetic of bovine serum albumin (BSA) from HyA hydrogels (3wt% with 100% crosslinked without heparin) was measured (Supplementary Fig 5b).

2.5. Cell Culture, Cell Viability, Adhesion and Proliferation

The $GFP^+/Sca\text{-}1^+/CD105^+/CD45^-$ CPCs were isolated and cultured in Iscove's Modified Dulbecco's Medium(IMDM) basal media containing 10% Fetal bovine serum (FBS) and 1% Penicillin-Streptomycin (PS) as previously described [10]. For cell encapsulation in the HyA hydrogels, confluent cells were trypsinized, collected cells were encapsulated density of 5×10^6 cells/mL in HyA hydrogel. Before adding the cell culture media, cell-gel constructs were incubated for 30 minutes at 37 °C to allow sufficient crosslinking to occur for gelation. Cell viability in the hydrogel was assessed by a Live/Dead staining kit (Invitrogen), and cell attachment was characterized by F-actin staining. Cell proliferation inside the hydrogels was quantified using the Alamar blue assay [38, 39]. Tubule quantification was performed on z-stacked confocal images of CD31 staining using FIJI (National Institutes of Health, Bethesda, MD). Before processing the images on FIJI, single color image z-stack were stitched together and converted to an 8-bit RGB stack, and noise outliers were removed. Results are reported as the average of three imaging locations in each sample.

2.6. Immunocytochemistry

For immunocytochemistry, hydrogel samples were fixed using 4% (v/v) paraformaldehyde for 30 min and permeabilized with 0.1% Triton X-100 for 5 min. After blocking with 3% BSA for 1 hr, hydrogel samples were incubated overnight at 4°C with a 1:200 dilution of primary antibody (rabbit anti-CD31 IgG). After washing the cells 3x with PBS, hydrogel samples were incubated with a 1:200 dilution of goat anti-rabbit AlexaFluor Texas red IgG (Invitrogen, Molecular Probes) for 2 h at RT. Prior to imaging, cell nuclei were stained DAPI for 5 min at RT. Cell-gel constructs were visualized using a Prairie two photon/ confocal microscope (Prairie Technologies, Middleton, WI).

2.7. Response Surface methodology

Data collected from the CPC proliferation and tubule quantification was transformed into a response surface by fitting the nine data points to a quadratic response surface with respect

to two factors: stiffness of matrix and RGD concentration. JMP statistical software (SAS, North Carolina, USA) was used to fit the quadratic equation using least squares regression.

2.8. Flow Cytometry

Cells entrained within the hydrogels were fixed with 4% paraformaldehyde for 30 min and permeabilized with 0.1% Triton for 5 min. After blocking with Fc-isotope controls for 10 min, the cells were stained with Allophycocyanin (APC)-conjugated anti-CD31 (PECAM-1) antibody or APC-conjugated anti-CD144 (VE-cadherin) antibody at 1:100 dilution for 1hr in dark. The hydrogels were then degraded by incubating them with 100 unit/mL hyaluronidase for 4hr to release the encapsulated cells. The stained cells were then pelleted by centrifugation, rinsed twice in PBS, passed through a 36-μm mesh cell strainer, and analyzed using a FC500 FACS Vantage cell sorter (BD Biosciences; see Supplementary Fig S6a, b).

2.9. Mouse Angiogenesis Protein Profiler Array

To measure the effect of the hydrogel on the expression of angiogenesis factors, we prepared hydrogels with entrained CPCs as described previously. After 12 days the supernatant was removed and retained for analysis. To measure the concentration of angiogenic factors that were expressed by the CPCs and retained within the matrix, the hydrogels were first washed with PBS and then degraded by the addition of hyaluronidase (100 unit/mL) at 37°C for 6 hr. Subsequently, the degraded hydrogels were incubated with heparinase I, II & III (2.5 unit/mL each) at 37°C for another 6 hr to eliminate heparin binding with the sequestered proteins. Next, the degraded hydrogels were centrifuged and the supernatant was collected for measurement of sequestered proteins in the hydrogels. The synthesized endogenous angiogenesis-associated proteins by the CPCs were measured using a mouse angiogenesis protein profiler array (R&D Systems, Minneapolis, MN) following the manufacturer's instructions.

In these experiments, an additional control was included consisting of HyA-P with soluble TGFβ1 at an equivalent concentration as the HyA-PHT hydrogels. The array was visualized by a chemiluminiscence substrate using Bio-Rad ChemiDoc XRS System. The relative expression of the angiogenesis proteins produced by the CPCs in each of the hydrogels was measured by comparing the pixel density of each chemiluminiscence image (Fig 5a, b).

2.10. Transduction of firefly luciferase (fLuc) into CPCs

Lentiviral vectors were packaged as previously described [40]. Briefly, third generation vectors were packaged by transient transfection of 293T cells cultured in IMDM media, supplemented with 10% FBS and 1% PennStrep, using a calcium phosphate precipitation protocol with 10 ug of a lentiviral transfer vector encoding firefly luciferase under the human ubiquitin promoter (hUb-fLuc), 5 ug of pMDLg/pRRE, 1.5 ug of pRSV Rev, and 3.5ug of pcDNA IVS VSV-G. Culture medium was changed 12h post-transfection, and viral supernatant was recovered 48h and 72h post-transfection and filtered using a 0.45um filter. Viral particles were concentrated via ultracentrifugation and resuspended in PBS.

CPC's were stably transduced with concentrated viral particles at a multiplicity of infection (MOI) of ~3 and culture medium was changed 24h post-transduction. Luciferase activity

was assayed in vitro with the Firefly Luciferase Assay System (Promega) by using a single-sample illuminometer (70% sensitivity, 2s measurement delay, 10s measurement read).

2.11. *In vivo* implantation study

To evaluate the ability of HyA based hydrogels to promote CPC survival and their ability to direct cell fate *in vivo*, a CPC/hydrogel suspension (100 μL) containing firefly luciferase (fLuc) transducted CPCs (5 millions cells/mL) was injected into the subcutaneous region of the anterior tibialis of syngeneic C57BL/6 mice. As a control, an equivalent concentration and volume of CPCs suspended in PBS was also was injected into the subcutaneous region of the anterior tibialis of syngeneic C57BL/6 mice. *In vivo* cell proliferation and survival was assessed at predetermined time point on the basis of the measured radiance ($p/s/cm^2/SR$) of the bioluminescent implants. To evaluate the vascular relationship of host and implant, cardiac perfusion of AF568-conjugated isolectin GS-IB4 from Griffonia simplicifolia (Invitrogen) was performed on the implanted mice. To examine the implants for matrix production and neovascular response, explants were harvested and fixed in 4% paraformaldehyde, cryosectioned, and examined with two-photon confocal microscope (Prairie Technologies, Middleton, WI).

2.12. Statistical analysis

All quantitative measurements were performed on at least triplicate sIPNs. All values are expressed as means ± standard deviations (SD). One-way ANOVA with *post-hoc* Tukey tests were used to compare treatment groups in the quantitative measurements and $p<0.05$ was used to assess statistical significance.

3.0. Results

3.1. Defined material parameters were achieved using Acrylated HyA (AcHyA) hydrogel synthesis

For this study, two discrete macromers were synthesized: AcHyA conjugated with the cell adhesion peptide bsp-RGD(15) (**AcHyA-RGD**) [41] and AcHyA conjugated with the glycosaminoglycan heparin (**AcHyA-Heparin**) (Supplementary Fig. S1 and S2 for detailed synthesis and characterization of AcHyA components). The adhesion peptide was chosen based on a screen of seven peptides that are known to promote integrin engagement, cell adhesion and proliferation of cardiac progenitor cells (Supplementary Fig. S3). HyA hydrogels with a range of biochemical and physical parameters (Supplementary Table S1) were made by *in situ* crosslinking of AcHyA components (AcHyA-RGD, AcHyA-Heparin) via the Michael-type addition reaction with short matrix metalloproteinase (MMP-13) degradable peptide sequences presenting terminal cysteine residues (Fig. 1a, 1b). Gelation of the 3 wt.% hydrogel with 100% crosslinking density (defined as moles of thiol on the peptide crosslinker to moles of acrylate groups on the AcHyA) was initiated after approximately 60 seconds and was completed within 15 min, as determined by a time-sweep at 0.1% strain and 1 Hz using an oscillatory rheometer (Fig. 1c). The viscoelastic properties, gelation kinetics, mass swelling ratios (Q_m), and sol fractions of the resulting hydrogels were dependent on both the weight percentage of AcHyA and the MMP crosslinking density (Supplementary Fig. S4). Importantly, low sol fraction of HyA hydrogels indicates a higher

relative efficiency of HyA crosslinking in the network, and that they were highly hydrolytically stable.

Retention kinetics of growth factors within the aforementioned HyA hydrogels was controlled by the relative ratio of exogenously added growth factor and heparin in the hydrogel (Supplementary Fig. S5) [28–30]. Added TGFβ1 in the hydrogel associate with the heparin via a non-covalent, charge-dependent interaction. Initial loading, release rate and retention at day 21 was dependent on heparin content and TGFβ1 concentration in the hydrogels (Supplementary Table S2). For example, covalent conjugation of 0.03 wt.% heparin in the HyA network retained 70% of TGFβ1 within the hydrogel for 21 days (Fig. 1d). HyA hydrogels without heparin retained less than 30% of the exogenously added TGFβ1 after 12 days, and a highly negatively charged protein BSA was completely released from the HyA hydrogel (3wt% with 100% crosslinking without heparin) within 72 hours. The mechanism for growth factor retention was, therefore, a combination of TGFβ1 binding directly with heparin via the protein's heparin-binding domain, and charge association between the oppositely charged growth factor and HyA[28, 29] (Fig. 1d and Supplementary Fig S5b).

3.2. CPC adhesion and proliferation was dependent on the AcHyA hydrogel parameters

To evaluate the effect of each AcHyA component on CPC survival, adhesion, and proliferation, four formulations of HyA hydrogels were synthesized: (1) AcHyA only (**HyA**); (2) AcHyA and AcHyA-RGD (**HyA-P**); (3) AcHyA, AcHyA-RGD and AcHyA-Heparin (**HyA-PH**); and, (4) AcHyA, AcHyA-RGD and AcHyA-Heparin-TGFβ1 (**HyA-PHT**). All four hydrogel combinations contained 3wt% AcHyA with 100% crosslinking, which yielded a shear storage modulus of 850Pa. For these experiments, the bsp-RGD(15) peptide, heparin, and TGFβ1 concentrations were 380 μM, 11.4 μg/μl, and 40 nM TGFβ1, respectively, and were chose based on previous reports [28, 37, 42–44]. Minimal (<5%) CPC death was observed in each of the hydrogels, independent of the combination of components used (Fig 2). CPCs seeded within all three hydrogels containing AcHyA-RGD exhibited robust spreading and elongated cellular morphology, whereas CPCs seeded in the hydrogel containing only HyA remained rounded and did not assume typical adherent cell morphology (Fig. 2a). We calculated the area of CPC spreading in the hydrogels and found the cells in HyA-PHT spread the most (1600 μm^2). However, the relative difference in cell area for any of the hydrogels containing AcHyA-RGD was small compared to the area of rounded cells in the HyA hydrogel (660 μm^2, Fig. 2b).

The proliferation of CPCs in the same four hydrogels was quantified over 21 days (Fig. 2c). Statistically, there was no significant difference between any of the gels at Days 3 and 7, and only marginal proliferation was observed in the HyA hydrogel through day 21. By contrast, CPCs proliferated consistently from day 3 to day 21 in all three hydrogels containing AcHyA-RGD (i.e., HyA, HyA-PH and HyA-PHT). At day 14, HyA was significantly less than HyA-PH and HyA-PHT, and at day 21, both HyA and HyA-P were significantly less than the heparin-containing HyA-PH and HyA-PHT hydrogels ($p<0.05$).

These results reveal that the adhesion peptide bsp-RGD(15) was required for CPC function in the AcHyA hydrogels, and the additional with heparin further enhanced the proliferation

of CPCs. The HyA-PHT hydrogel was used to evaluate the effect of bsp-RGD(15) density and hydrogel stiffness on CPC proliferation using response surface methodology (**RSM**) to analyze the multiparametric data (Fig. 3). CPC proliferation was linearly dependent on bsp-RGD (15) density within the range evaluated, whereas the effect of hydrogel stiffness was maximum at approximately 800 Pa. Furthermore, the matrix stiffness had greater influence on the proliferation rate of the CPCs compared to peptide density, as the former appeared to dominate the response surfaces at every time point.

3.3. CPC formation into endothelial networks was controlled via AcHyA hydrogel parameters

The Sca-1^+/$CD45^-$ population of CPCs readily differentiate into endothelial cells under the appropriate induction conditions [10]. In this study, differentiation of Sca-1^+/$CD45^-$ population of CPCs into endothelial cells within the hydrogels was measured by immunostaining for CD31 and uptake of acetylated low-density lipoprotein (Ac-LDL) (Fig. 4a), and quantified by flow cytometry for the EC-specific markers CD31 and VE-Cadherin. We studied the four formulations of HyA hydrogels used in the adhesion and proliferation studies and found all of the HyA gels containing bsp-RGD (15) significantly increased the expression of both EC markers ($p<0.05$: Supplementary Fig. S6a). Inclusion of TGFβ1 increased the number of cells expressing CD31 relative to the HyA-P hydrogels, and also increased the number of cells expressing VE-cadherin relative to both the HyA-P and HyA-PH hydrogels. For CPCs in the HyA-PHT hydrogels, the expression of CD31 and VE cadherin increased significantly from days 3–12 ($p<0.05$, Supplementary Fig. S6b), and a tubular network formed on day 6, which increased in density and complexity through day 12 (Supplementary Fig. S6c). Interestingly, the cellular network formation was only observed in HyA-PHT hydrogels (Fig. 4a), which indicated exogenous TGFβ1 presented in the network induced the tubule network formation, consistent with previous investigations demonstrating the role of TGFβ1 to promote capillary tube formation by CPCs [44] and endothelial cells [45] in two-dimensional experiments.

To decouple the effect of heparin and TGFβ1, we included control HyA-P hydrogels containing an equivalent concentration of soluble TGFβ1 as the HyA-PHT hydrogel either in the media or polymerized within the gel. Tubular network formation was not evident in either HyA-P ‘soluble’ containing TGFβ1 gels compared to HyA-PHT hydrogel (Fig. 4a, & Supplementary Fig. S10, S11). Therefore, the presentation of TGFβ1 by heparin substantially enhanced the network formation process, as an equimolar concentration of TGFβ1 supplied as a soluble mediator in HyA-hydrogels lacking heparin was insufficient to generate a similar response.

Among the four hydrogels tested, the HyA-PHT was the only one that supported substantial cell proliferation, endothelial cell differentiation, and tubular network formation in the hydrogel, therefore, the HyA-PHT hydrogel was chosen to further study the effect of matrix modulus and peptide density on tube network formation, see Supplementary table S1 for the concentration ranges used for each of these components. After culture for 12 days in HyA-PHT hydrogels, formation of tubular networks was dependent on both hydrogel modulus and peptide density (Fig. 4b). Response of total tubule length to the bsp-RGD (15) peptide

density was approximately linear within the range evaluated in this study. Similarly, the thickness of the tubules formed in HyA-PHT hydrogels exhibited a linear response to both hydrogel modulus and bsp-RGD (15) peptide density, although this tubule characteristic was more sensitive to the matrix stiffness parameter (Fig. 4c and d). These complex three-dimensional networks (Fig. 4e), which appeared to contain a central lumen (Fig. 4f), suggested that CPCs in the HyA-PHT hydrogels were capable of forming nascent vessels *in vitro*.

3.4. The AcHyA hydrogels encouraged CPCs to produce angiogenic cytokine

The effect of hydrogel components on CPC paracrine function was also investigated. CPCs were cultured for 12 days in the four HyA hydrogel combinations previously described (i.e., HyA, HyA-P, HyA-PH and HyA-PHT) and the concentration of secreted angiogenic factors retained by the hydrogel matrix were measured (Fig. 5). Only low paracrine factor expression was observed by CPCs entrained in any of the hydrogels without TGFβ1, and by contrast, the cells seeded in the HyA-PHT expressed high levels of angiogenic factors, including those stimulating vascular stabilization (Fig. 5a), which were retained within the matrix at 12 days. By contrast, the cells seeded in HyA-P and treated with soluble TGFβ1 stimulated a limited subset of paracrine factors (Fig. 5b), where the expression levels in both the hydrogel and supernatant were lower relative to the HyA-PHT hydrogels.

3.5. The AcHyA hydrogels enhance CPC survival and neovascularization *in vivo*

The *in vivo* performance of the hydrogels in promoting CPC survival, differentiation, and engraftment was evaluated using a subcutaneous implantation model in syngeneic C57BL/6 mice. The CPCs were transduced with a constitutive firefly luciferase (fLuc) reporter to evaluate cell survival for over 30 days after implantation (Fig. 6a). CPCs entrained in the HyA, HyA-PH, HyA-PHT hydrogels experienced a drop in bioluminescence (BLI) signal after 4 days, followed by a steady increase in BLI signal from day 4 to day 32 (Fig. 6b). The early drop in BLI signal was anticipated due to the likely activity that occurs on the ubiquitin promoter as the CPCs recover from initial proteotoxic stresses encountered following *in vivo* implantation [46, 47]. An overall lower BLI signal from the control CPCs injected with either HyA or HyA-PH indicated fewer cells survived in these matrices, while a more dramatic drop in BLI signal from CPCs injected with saline never recovered, consistent with previous reports indicating rapid death and clearance of cells that were transplanted in the absence of a supporting matrix [9, 48](Fig. 6b).

After 32 days, mice were sacrificed and the transplanted regions were inspected. In the limbs injected with hydrogels (HyA, HyA-PH, and HyA-PHT), the implant could be readily identified in the subcutaneous tissue (Fig. 6c). Immunohistochemistry analysis of the all the hydrogel groups exhibited a high cellular density, and many of the entrained cells were GFP^+ (Fig. 6d), indicating that they were derived from the GFP^+ CPCs. GFP^+ CPCs were not observed at the site of saline injection (Supplementary Fig. S7). Extracellular matrix production was evaluated within and around the hydrogel implants using Masson's trichrome stain and immunohistochemical staining for Type IV collagen (Fig. 7a, Supplementary Fig. S9). The Masson's trichome demonstrated a mesh-like network of secreted collagen matrix throughout the HyA-PHT explants, while substantially less

collagen staining was observed in the HyA or HyA-PH hydrogels. Furthermore, the ECM formed within the HyA-PHT hydrogels was rich with Type IV collagen, which is typically associated with basal lamina, and the Type IV collagen was arranged into tubule structures, suggesting the implanted cells had coordinated extracellular matrix remodeling in the hydrogel to form nascent vascular structures. It is noteworthy that the other hydrogels tested, HyA and HyA-PH, were comparable in size to the HyA-PHT gels when initially explanted at day 32. However, some hydrogel was shed from the HyA and HyA-PH specimens during cryosectioning due to the low amount of matrix formation supported by these materials and therefore do not appear in the immunohistochemistry.

Endothelial cell differentiation was also verified in the hydrogel implants, as the majority of the cells were positive for $CD31^+$ (Fig. 6d, Supplementary Fig. 8). Vessel stabilization was attributed to pericytes,[49, 50] and their presence within the hydrogel implants was detected by immunostainin for the pericyte marker neuron-glial antigen 2 (NG2; Fig 6d, Supplementary Fig. 8). Only HyA-PHT implants demonstrated infiltration of pericyte cells from the host tissue to implants, as the $NG2^+$ cells intermingled with GFP^+ donor cells [49, 50]. Endomucin staining confirmed the presence of a robust vasculature, further demonstrating the enhanced vascularization within the HyA-PHT hydrogel implants,. By comparison, the HyA and HyA-PH explants demonstrated minimal vascularization on the basis of endomucin staining. Finally, the explants were stained with the Alexa Fluor 568-conjugated GS-IB4 lectin via systemic perfusion through the host vasculature. Vascular structures were clearly visible in HyA-PHT explants with cross sectional areas ranging from 100 to 30,000 μm^2 (Fig. 7a and 7b, Supplementary Fig. 9). Negligible vasculature could be discerned in the other HyA treatments after perfusion of AF-568 GS-IB4 lectin or endomucin staining. Thus, cells in the HyA-PHT hydrogels encouraged significant enhancement of vascular development in the implant, and most significantly the vasculature anastomosed with the host's circulatory system (Fig. 7a and 7b, Supplementary Fig. 9). Collectively, these observations indicated that MACT with the HyA-PHT implant relative to HyA and HyA-PH promoted a superior level of neovascularization with vessels that spontaneously anastomosed with the host vasculature, which were also superior relative to previously used biomaterials [28, 30, 51–53].

4.0. Discussion

In this study, a tunable approach to HyA hydrogel synthesis enabled a comprehensive investigation into gel properties that efficiently supported donor cell survival during transplantation and encouraged integration into the host tissue. We employed a modular method of HyA hydrogel synthesis that enabled independent control over both mechanical properties and biological features including: the density of peptide sequences for cell attachment via binding of integrin receptors; and, sequestration of exogenously added or endogenously synthesized growth factors via conjugated heparin. While similar systematic approaches and synthetic hydrogel matrices have been proposed for clinical use [22, 24, 54], they have been synthesized using methods in which crosslinking molecules are necessarily put in competition with other biological agents for binding sites on the biopolymers. As a result, their mechanical properties were inversely dependent on the density of conjugated molecules used to functionalize the material. By contrast, the mechanical properties, mass

swelling ratio (Q_m) and sol fraction of the hydrogel system developed in this work were dependent on both total weight percentage of HyA and the concentration of peptide crosslinkers (Supplementary Fig. S4), but independent of the biological features that were incorporated on the other AcHyA hydrogel components. With this approach it was possible to overcome several limitations previously reported for MACT systems[22, 24, 55] such as: (1) compromised crosslinking efficiencies due to competition between macromer chains and other bioactive moieties in the hydrogel network; and, (2) unpolymerized soluble adhesion ligands entrained in the material acting as antagonists [22, 24]. Significantly, the material design space was not constrained by any dependencies between the hydrogel components (Supplementary Table S1), and therefore we could evaluate different HyA-hydrogels based on first-principles of cell-material interactions without limitations imposed by the method of synthesis.

Exogenous TGFβ1 was used in this study based on its role in promoting capillary tube formation by CPCs [44] and endothelial cells [45]. Based on previous work [27, 56, 57], we anticipated that presentation of TGFβ1 by heparin would substantially facilitate its function by retaining it in an active form and in close proximity to the donor CPCs. Our findings confirmed the significance of the covalently conjugated heparin component of the HyA hydrogels to direct cell function [29, 58, 59], as an equimolar concentration of TGFβ1 supplied as a soluble mediator either within or external to HyA-P hydrogels lacking heparin was insufficient to generate a similar network formation response, as revealed by lower CD31 expression and Ac-LDL uptake (Fig. 4; Supplementary Figs. S10 & S11). By contrast, the HyA-PHT hydrogels promoted the formation of a robust network, and this observation depended not only on TGFβ1's presence, but also on the solid phase presentation of TGFβ1 via its heparin-binding domain through electrostatic interactions [60]. Heparin association is known to protect growth factors from proteolytic degradation, enable growth factor prolonged bioactivity, and act as a co-receptor for growth factors to exert their biological effects on stem cells [28, 29].

We further observed that the heparin retained angiogenic factors that were expressed by the entrained CPCs that exhibited either a heparin-binding domain and/or a basic isoelectric point (e.g., IGFBP-2, 3, CXCL16, Serpin F1 & E1, Endostatin, IL10, IP10; Fig. 5). Significantly, we demonstrated that addition of heparin in the HyA hydrogels was necessary to coordinate the presentation of exogenously added TGFβ1 and to support the trophic functions of the CPCs by sequestering multiple secreted angiogenic factors within the matrix. These sequestered growth factors were presented by within the crosslinked polymer (i.e., solid phase), thereby enhancing their effectiveness in the hydrogel. The net result was retention and solid phase presentation of a wide array of angiogenic growth factors within the hydrogel, which enabled a prolonged bioactive effect on the entrained CPCs.

In vivo, we demonstrated that HyA hydrogels carrying electrostatically bound TGFβ1 through covalently conjugated heparin (HyA-PHT) promoted the highest cell survival, endothelial cell differentiation, and robust ECM development when implanted into murine hindlimbs. These hydrogels encouraged vascular development in the implant, and most significantly the vasculature anastomosed with the host's circulatory system (Fig. 6, 7, and Supplementary Fig. 8, 9). Thus, further engineering of the heparin component of the HyA-

PHT hydrogels will be key to tuning their performance to promote stem cell survival and function for specific MACT applications.

Although the overall approach in this study was focused on CPC transplantation, these HyA hydrogels were designed for easy adaptation for other cell types and therapeutic applications. Integration of transplanted cells with a host's vasculature is nearly a universal challenge following cell transplantation, and the heparin-containing HyA hydrogels have immense promise in a variety of MACT applications. Given the wide range of biological and mechanical parameters for these HyA hydrogels, it will be possible to engineer a matrix that promotes additional specific functions of donor cells to enhance their therapeutic potential. Therefore, we anticipate these biomaterials will be an enabling technology to improve the clinical outcomes for cell translation therapies.

5.0. Conclusion

We developed a system of hyaluronic acid (**HyA**)-based hydrogels and determined the role of the hydrogel components to promote Sca-1^+/$CD45^-$ **CPCs** cell survival, adhesion, endothelial cell differentiation and tubule formation. The addition of heparin in the HyA hydrogels was necessary to coordinate the presentation of TGFβ1 and support the trophic functions of the CPCs by sequestering multiple endogenously secreted angiogenic factors. These HyA hydrogels also promoted *in vivo* CPC survival after implantation into subcutaneous murine hind-limbs and encouraged their participation in the ensuing neovascular response, including blood vessels that anastomosed with the host's blood vessels. These findings illustrate that hydrogels that sequester both exogenously added and endogenously synthesized growth factors is a promising strategy for improving survival of transplanted progenitor cells.

Supplementary Material

Refer to Web version on PubMed Central for supplementary material.

Acknowledgments

This work was supported in part by National Heart Lung and Blood Institute of the National Institutes of Health R01HL096525 (K.E.H.), and the Siebel Stem Cell Institute Postdoctoral Fellowship (A.K.J.). Isolation and characterization of cloned Sca-1^+/$CD45^-$ cells was supported in part by UCSF Translational Cardiac Stem Cell Program, the Leone-Perkins Foundation, and by the Torian Foundation and the Vadasz Foundation (Y.Y.). We wish to thank Derek Dashti and Pamela Tiet for their assistance with cell culture and image analysis, Natalie C. Marks for her assistance with flow cytometry analysis, and Kimberly Kam for her assistance with the adhesion peptide assays. We would also like to acknowledge Hector Nolla from the UC Berkeley Flow Cytometry Center for his assistance with flow cytometry instrumentation, Dr. Mary West from the QB3 Shared Stem Cell Facility for her assistance with confocal imaging, and Dr. Jeffrey Pelton from the QB3-Berkeley Core Research Facility for his assistance with ^{1}H proton NMR.

References

1. Min J-Y, Sullivan MF, Yang Y, Zhang J-P, Converso KL, Morgan JP, et al. Significant improvement of heart function by cotransplantation of human mesenchymal stem cells and fetal cardiomyocytes in post-infarcted pigs. Ann Thorac Surg. 2002; 74:1568–75. [PubMed: 12440610]

2. Matsuura K, Honda A, Nagai T, Fukushima N, Iwanaga K, Tokunaga M, et al. Transplantation of cardiac progenitor cells ameliorates cardiac dysfunction after myocardial infarction in mice. The Journal of Clinical Investigation. 2009; 119:2204–17. [PubMed: 19620770]

3. Mizuno Y, Chang H, Umeda K, Niwa A, Iwasa T, Awaya T, et al. Generation of skeletal muscle stem/progenitor cells from murine induced pluripotent stem cells. FASEB. 2010; 24:2245–53.

4. Liu H, Kim Y, Sharkis S, Marchionni L, Jang YY. In vivo liver regeneration potential of human induced pluripotent stem cells from diverse origins. Science Translational Medicine. 2011; 3:82ra39.

5. Toma C, Pittenger MF, Cahill KS, Byrne BJ, Kessler PD. Human mesenchymal stem cells differentiate to a cardiomyocyte phenotype in the adult murine heart. Circulation. 2002; 105:93–8. [PubMed: 11772882]

6. Beauchamp JR, Morgan JE, Pagel CN, Partridge TA. Dynamics of myoblast transplantation reveal a discrete minority of precursors with stem cell-like properties as the myogenic source. J Cell Biol. 1999; 144:1113–22. [PubMed: 10087257]

7. Mitkari B, Kerkela E, Nystedt J, Korhonen M, Mikkonen V, Huhtala T, et al. Intra-arterial infusion of human bone marrow-derived mesenchymal stem cells results in transient localization in the brain after cerebral ischemia in rats. Experimental Neurology. 2013; 239:158–62. [PubMed: 23059455]

8. Mora-Lee S, Sirerol-Piquer MS, Gutierrez-Perez M, Gomez-Pinedo U, Roobrouck VD, Lopez T, et al. Therapeutic effects of hMAPC and hMSC transplantation after stroke in mice. PLoS ONE. 2012; 7:e43683. [PubMed: 22952736]

9. Li Z, Wu JC, Sheikh AY, Kraft D, Cao F, Xie X, et al. Differentiation, survival, and function of embryonic stem cell derived endothelial cells for ischemic heart disease. Circulation. 2007; 116:I46–54. [PubMed: 17846325]

10. Ye J, Boyle A, Shih H, Sievers RE, Zhang Y, Prasad M, et al. Sca-1+ Cardiosphere-Derived Cells Are Enriched for Isl1-Expressing Cardiac Precursors and Improve Cardiac Function after Myocardial Injury. PLoS ONE. 2012; 7:e30329. [PubMed: 22272337]

11. Horie N, Pereira MP, Niizuma K, Sun G, Keren-Gill H, Encarnacion A, et al. Transplanted stem cell-secreted vascular endothelial growth factor effects poststroke recovery, inflammation, and vascular repair. Stem Cells. 2011; 29:274–85. [PubMed: 21732485]

12. Mureli S, Gans CP, Bare DJ, Geenen DL, Kumar NM, Banach K. Mesenchymal stem cells improve cardiac conduction by upregulation of connexin 43 through paracrine signaling. American Journal of Physiology - Heart and Circulatory Physiology. 2013; 304:H600–H9. [PubMed: 23241322]

13. Prestwich GD. Engineering a clinically-useful matrix for cell therapy. Organogenesis. 2008; 4:42–7. [PubMed: 19279714]

14. Prestwich GD. Delivery, retention and engraftment of progenitor cells in cell therapy. Biomatter. 2013; 3:pii, e24549.

15. Prestwich GD, Erickson IE, Zarembinski TI, West M, Tew WP. The translational imperative: making cell therapy simple and effective. Acta Biomater. 2012; 8:4200–7. [PubMed: 22776825]

16. Gao J, Liu R, Wu J, Liu Z, Li J, Zhou J, et al. The use of chitosan based hydrogel for enhancing the therapeutic benefits of adipose-derived MSCs for acute kidney injury. Biomaterials. 2012; 33:3673–81. [PubMed: 22361096]

17. Lesman A, Habib M, Caspi O, Gepstein A, Arbel G, Levenberg S, et al. Transplantation of a tissue-engineered human vascularized cardiac muscle. Tissue Engineering Part A. 2010; 16:115–25. [PubMed: 19642856]

18. Parisi-Amon A, Mulyasasmita W, Chung C, Heilshorn SC. Protein-engineered injectable hydrogel to improve retention of transplanted adipose-derived stem cells. Advanced Healthcare Materials. 2013; 2:428–32. [PubMed: 23184882]

19. Xiong Q, Hill KL, Li Q, Suntharalingam P, Mansoor A, Wang X, et al. A fibrin patch-based enhanced delivery of human embryonic stem cell-derived vascular cell transplantation in a porcine model of postinfarction left ventricular remodeling. Stem Cells. 2011; 29:367–75. [PubMed: 21732493]

20. Unterman SA, Gibson M, Lee JH, Crist J, Chansakul T, Yang EC, et al. Hyaluronic acid-binding scaffold for articular cartilage repair. Tissue Engineering Part A. 2012; 18:2497–506. [PubMed: 22724901]
21. Wall ST, Yeh CC, Tu RY, Mann MJ, Healy KE. Biomimetic matrices for myocardial stabilization and stem cell transplantation. J Biomed Mater Res A. 2010; 95:1055–66. [PubMed: 20878934]
22. Kim J, Kim IS, Cho TH, Lee KB, Hwang SJ, Tae G, et al. Bone regeneration using hyaluronic acid-based hydrogel with bone morphogenic protein-2 and human mesenchymal stem cells. Biomaterials. 2007; 28:1830–7. [PubMed: 17208295]
23. Freudenberg U, Hermann A, Welzel PB, Stirl K, Schwarz SC, Grimmer M, et al. A star-PEG-heparin hydrogel platform to aid cell replacement therapies for neurodegenerative diseases. Biomaterials. 2009; 30:5049–60. [PubMed: 19560816]
24. Khetan S, Katz JS, Burdick JA. Sequential crosslinking to control cellular spreading in 3-dimensional hydrogels. Soft Matter. 2009; 5:1601–6.
25. Raeber GP, Lutolf MP, Hubbell JA. Molecularly engineered peg hydrogels: a novel model system for proteolytically mediated cell migration. Biophysical Journal. 2005; 89:1374–88. [PubMed: 15923238]
26. Craig EA, Parker P, Austin AF, Barnett JV, Camenisch TD. Involvement of the MEKK1 signaling pathway in the regulation of epicardial cell behavior by hyaluronan. Cellular Signaling. 2010; 22:968–76.
27. Sakiyama-Elbert SE, Hubbell JA. Controlled release of nerve growth factor from a heparin-containing fibrin-based cell ingrowth matrix. J Control Release. 2000; 69:149–58. [PubMed: 11018553]
28. Pike DB, Cai S, Pomraning KR, Firpo MA, Fisher RJ, Shu XZ, et al. Heparin-regulated release of growth factors in vitro and angiogenic response in vivo to implanted hyaluronan hydrogels containing VEGF and bFGF. Biomaterials. 2006; 27:5242–51. [PubMed: 16806456]
29. Sakiyama-Elbert SE, Hubbell JA. Development of fibrin derivatives for controlled release of heparin-binding growth factors. J Control Release. 2000; 65:389–402. [PubMed: 10699297]
30. Cai S, Liu Y, Zheng Shu X, Prestwich GD. Injectable glycosaminoglycan hydrogels for controlled release of human basic fibroblast growth factor. Biomaterials. 2005; 26:6054–67. [PubMed: 15958243]
31. Yang J, Watkins D, Chen C-L, Bhushan B, Zhou Y, Besner GE. Heparin-binding epidermal growth factor-like growth factor and mesenchymal stem cells act synergistically to prevent experimental necrotizing enterocolitis. Journal of the American College of Surgeons. 2012; 215:534–45. [PubMed: 22819639]
32. Prokoph S, Chavakis E, Levental KR, Zieris A, Freudenberg U, Dimmeler S, et al. Sustained delivery of SDF-1alpha from heparin-based hydrogels to attract circulating pro-angiogenic cells. Biomaterials. 2012; 33:4792–800. [PubMed: 22483246]
33. Guan K, Hasenfuss G. Cardiac resident progenitor cells: evidence and functional significance. European Heart Journal. 2012
34. Jha AK, Hule RA, Jiao T, Teller SS, Clifton RJ, Duncan RL, et al. Structural analysis and mechanical characterization of hyaluronic acid-based doubly cross-linked networks. Macromolecules. 2009; 42:537–46. [PubMed: 20046226]
35. Jha AK, Malik MS, Farach-Carson MC, Duncan RL, Jia X. Hierarchically structured, hyaluronic acid-based hydrogel matrices via the covalent integration of microgels into macroscopic networks. Soft Matter. 2010; 6:5045–55. [PubMed: 20936090]
36. Tae G, Kim Y-J, Choi W-I, Kim M, Stayton PS, Hoffman AS. Formation of a novel heparin-based hydrogel in the presence of heparin-binding biomolecules. Biomacromolecules. 2007; 8:1979–86. [PubMed: 17511500]
37. Chung EH, Gilbert M, Virdi AS, Sena K, Sumner DR, Healy KE. Biomimetic artificial ECMs stimulate bone regeneration. J Biomed Mater Res A. 2006; 79:815–26. [PubMed: 16886222]
38. Voytik-Harbin S, Brightman A, Waisner B, Lamar C, Badylak S. Application and evaluation of the alamarblue assay for cell growth and survival of fibroblasts. In Vitro Cellular & Developmental Biology - Animal. 1998; 34:239–46. [PubMed: 9557942]

39. Al-Nasiry S, Geusens N, Hanssens M, Luyten C, Pijnenborg R. The use of Alamar Blue assay for quantitative analysis of viability, migration and invasion of choriocarcinoma cells. Human Reproduction. 2007; 22:1304–9. [PubMed: 17307808]
40. Yang L, Yang H, Rideout K, Cho T, Joo KI, Ziegler L, et al. Engineered lentivector targeting of dendritic cells for in vivo immunization. Nat Biotechnol. 2008; 26:326–34. [PubMed: 18297056]
41. Rezania A, Thomas CH, Branger AB, Waters CM, Healy KE. The detachment strength and morphology of bone cells contacting materials modified with a peptide sequence found within bone sialoprotein. Journal of Biomedical Materials Research. 1997; 37:9–19. [PubMed: 9335344]
42. Lei Y, Gojgini S, Lam J, Segura T. The spreading, migration and proliferation of mouse mesenchymal stem cells cultured inside hyaluronic acid hydrogels. Biomaterials. 2011; 32:39–47. [PubMed: 20933268]
43. Goumans M-J, Liu Z, ten Dijke P. TGF-[beta] signaling in vascular biology and dysfunction. Cell Res. 2009; 19:116–27. [PubMed: 19114994]
44. Goumans M-J, de Boer TP, Smits AM, van Laake LW, van Vliet P, Metz CHG, et al. TGF-beta1 induces efficient differentiation of human cardiomyocyte progenitor cells into functional cardiomyocytes in vitro. Stem Cell Research. 2008; 1:138–49. [PubMed: 19383394]
45. Bein K, Odell-Fiddler ET, Drinane M. Role of TGF-beta1 and JNK signaling in capillary tube patterning. American Journal of Physiology - Cell Physiology. 2004; 287:C1012–C22. [PubMed: 15201140]
46. Dantuma NP, Lindsten K. Stressing the ubiquitin-proteasome system. Cardiovascular Research. 2010; 85:263–71. [PubMed: 19633314]
47. Workman P, Davies FE. A stressful life (or death): combinatorial proteotoxic approaches to cancer-selective therapeutic vulnerability. Oncotarget. 2011; 2:277–80. [PubMed: 21515932]
48. Liu Z, Wang H, Wang Y, Lin Q, Yao A, Cao F, et al. The influence of chitosan hydrogel on stem cell engraftment, survival and homing in the ischemic myocardial microenvironment. Biomaterials. 2012; 33:3093–106. [PubMed: 22265788]
49. Armulik A, Abramsson A, Betsholtz C. Endothelial/pericyte interactions. Circulation Research. 2005; 97:512–23. [PubMed: 16166562]
50. You W-K, Yotsumoto F, Sakimura K, Adams R, Stallcup W. NG2 proteoglycan promotes tumor vascularization via integrin-dependent effects on pericyte function. Angiogenesis. 2013; 17:61–76. [PubMed: 23925489]
51. Hanjaya-Putra D, Bose V, Shen Y-I, Yee J, Khetan S, Fox-Talbot K, et al. Controlled activation of morphogenesis to generate a functional human microvasculature in a synthetic matrix. Blood. 2011; 118:804–15. [PubMed: 21527523]
52. Kusuma S, Shen Y-I, Hanjaya-Putra D, Mali P, Cheng L, Gerecht S. Self-organized vascular networks from human pluripotent stem cells in a synthetic matrix. Proceedings of the National Academy of Sciences. 2013; 110:12601–6.
53. Fujita M, Ishihara M, Simizu M, Obara K, Ishizuka T, Saito Y, et al. Vascularization in vivo caused by the controlled release of fibroblast growth factor-2 from an injectable chitosan/non-anticoagulant heparin hydrogel. Biomaterials. 2004; 25:699–706. [PubMed: 14607508]
54. Lutolf MP, Weber FE, Schmoekel HG, Schense JC, Kohler T, Muller R, et al. Repair of bone defects using synthetic mimetics of collagenous extracellular matrices. Nat Biotechnol. 2003; 21:513–8. [PubMed: 12704396]
55. Kraehenbuehl TP, Zammaretti P, Van der Vlies AJ, Schoenmakers RG, Lutolf MP, Jaconi ME, et al. Three-dimensional extracellular matrix-directed cardioprogenitor differentiation: Systematic modulation of a synthetic cell-responsive PEG-hydrogel. Biomaterials. 2008; 29:2757–66. [PubMed: 18396331]
56. Bratt-Leal AM, Nguyen AH, Hammersmith KA, Singh A, McDevitt TC. A microparticle approach to morphogen delivery within pluripotent stem cell aggregates. Biomaterials. 2013; 34:7227–35. [PubMed: 23827184]
57. Hudalla GA, Koepsel JT, Murphy WL. Surfaces that sequester serum-borne heparin amplify growth factor activity. Advanced Materials. 2011; 23:5415–8. [PubMed: 22028244]

58. Wood MD, MacEwan MR, French AR, Moore AM, Hunter DA, Mackinnon SE, et al. Fibrin matrices with affinity-based delivery systems and neurotrophic factors promote functional nerve regeneration. Biotechnol Bioeng. 2010; 106:970–9. [PubMed: 20589674]

59. Wood MD, Moore AM, Hunter DA, Tuffaha S, Borschel GH, Mackinnon SE, et al. Affinity-based release of glial-derived neurotrophic factor from fibrin matrices enhances sciatic nerve regeneration. Acta Biomater. 2009; 5:959–68. [PubMed: 19103514]

60. Martino MM, Briquez PS, Ranga A, Lutolf MP, Hubbell JA. Heparin-binding domain of fibrin(ogen) binds growth factors and promotes tissue repair when incorporated within a synthetic matrix. Proc Natl Acad Sci U S A. 2013; 110:4563–8. [PubMed: 23487783]

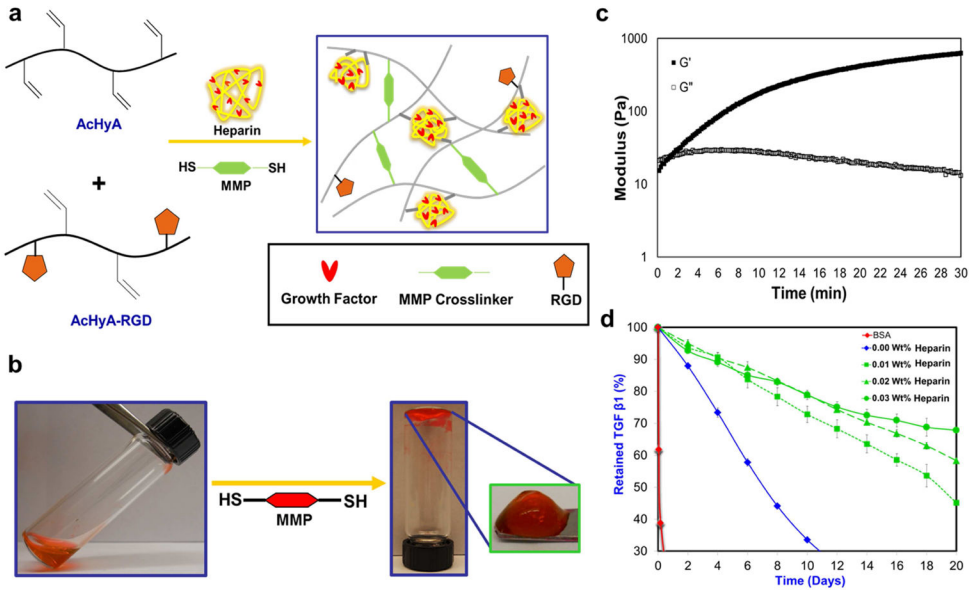

Figure 1. Schematic for gel synthesis

a, HyA hydrogels containing the cell adhesive bspRGD(15) peptide and heparin as a growth factor presenting agent were synthesized by using bis-cysteine matrix metalloproteinase (MMP)-degradable peptide crosslinkers that reacted via the Michael-type addition to acryl groups on the functionalized HyA precursors. **b,** Images of polymerized hydrogel – red dye is for fiduciary purposes. **c,** The time required to initiate gelation, defined when the storage modulus (G′) exceeds the loss modulus (G″) occurred within 60 seconds. Gelation was considered complete when G′ reached a plateau, and occurred within 15 minutes, depending on the weight ratio of HyA included in each hydrogel. **d,** Depending on the weight percentage of heparin present, HyA hydrogels (0.03 wt.% heparin) retain over 70% of the TGFβ1 for up to 20 days. Hydrogel with a lower wt% of heparin (e.g. 0.01wt.%) exhibitted a slow and nearly zero order release kinetics. Gels without heparin released most of the TGFβ1 by 10 days. There was minimum retention of BSA within the HyA hydrogels, which has acidic isoelectric point, confirming that molecular diffusion was not hindered by the crosslinking density of hydrogel.

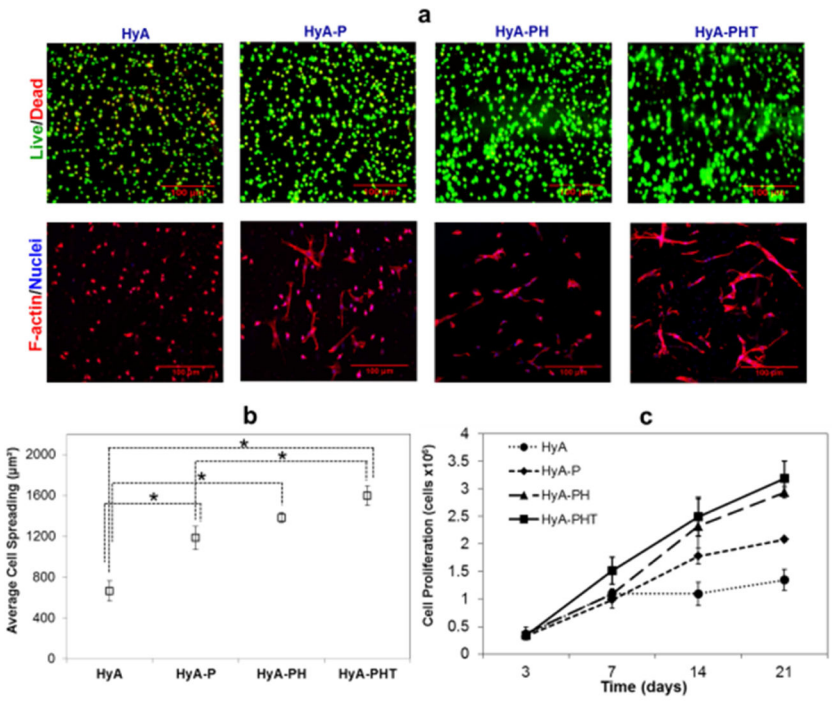

Figure 2. CPC Viability, proliferation, and adhesion in HyA hydrogels

(a, upper panels) The viability of CPCs encapsulated by the HyA-, HyA-P, HyA-PH and HyA-PHT hydrogels was high after one day of culture, as assessed by double staining with calcein (green, live cells) and propidium iodide (red, dead cells). **(a, lower panels)** CPCs were capable of adhering and spreading within the hydrogel networks containing the adhesive ligand bsp-RGD(15), as assessed by imaging for f-actin stress fibers (TRITC-phalloidin; red) and nuclei (DAPI; blue). **b** The area of spread cells was enhanced significantly by the addition of adhesion peptide and TGFβ1. **c** Cell proliferation within the HyA hydrogels was affected by the presence of heparin and TGFβ1, and at day 21, proliferation in both HyA and HyA-P were significantly less than HyA-PH and HyA-PHT hydrogels (ANOVA with Tukey, $p<0.05$).

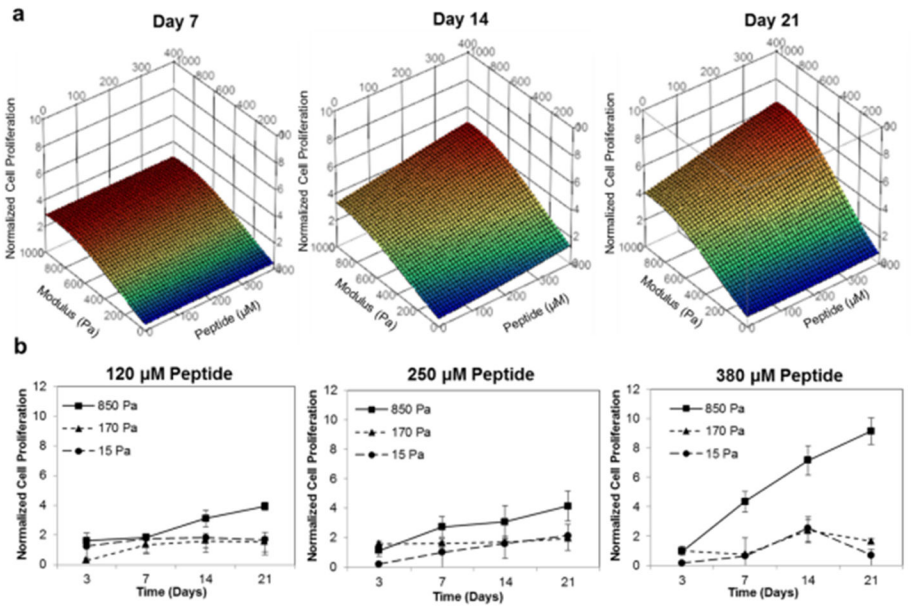

Figure 3. Dependency of cell proliferation on hydrogel stiffness and adhesion peptide density

a, RSM plots of CPC proliferation in HyA-PHT hydrogels with various moduli and concentrations (120–380 μM) of the cell adhesive ligand bsp-RGD (15). CPC proliferation was dose-dependent on the RGD density, and maximum at ~ 800 Pa. All data was normalized to the cell number (3.48×10^5) in hydrogels at day 3 data. **b,** Kinetic observations of CPC proliferation as a function of hydrogel stiffness in HyA-PHT hydrogels shown at three different bsp-RGD(15) densities.

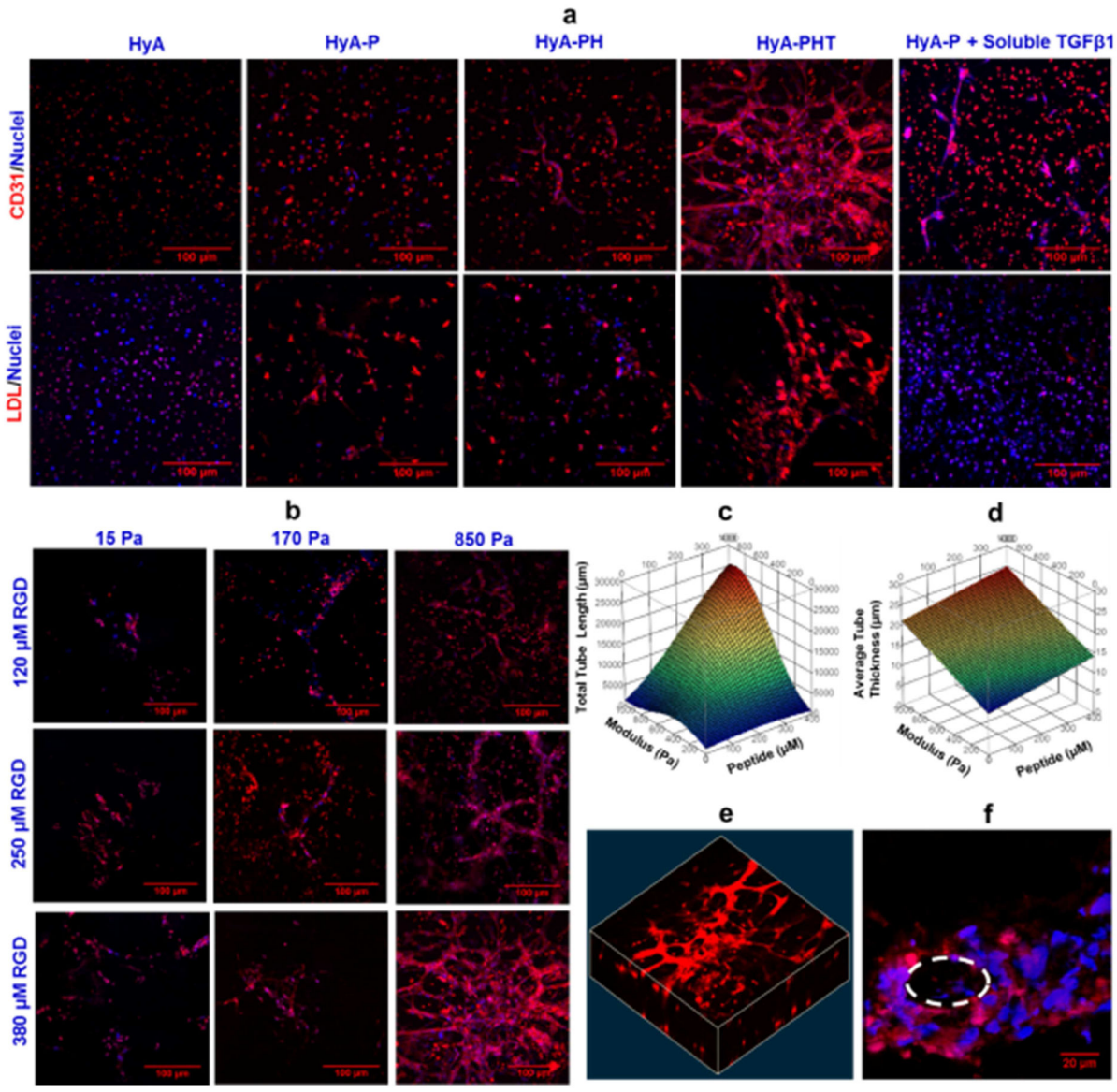

Figure 4. Validation of endothelial cell differentiation, and tube formation by CPCs was dependent on hydrogel stiffness and adhesion peptide density

a, Representative confocal microscopy images of immunostaining of endothelial cell marker CD31, and acetylated low-density lipoprotein (Ac-LDL) uptake by the cells after 12 days of culture in HyA, HyA-P, HyA-PH and HyA-PHT hydrogels. HyA-P treated with an equivalent concentration of soluble TGFβ1 as delivered in HyA-PHT was included as a control. Both TGFβ1 and heparin were necessary in the HyA hydrogels to promote endothelial cell differentiation, as determined by CD31 expression and Ac-LDL uptake, and tubule formation in HyA-PHT hydrogel (850Pa modulus, 380μM bsp-RGD(15), 0.03wt% heparin, and 40nM TGFβ1). **b,** Vascular-like tube formation of CD31 positive cells in the HyA-PHT hydrogel was observed as a function of bsp-RGD(15) peptide density (120–380 μM) and gel modulus (15–850 Pa). RSM plots of the combined effects of peptide ligand and material modulus on **c,** total tube length, and **d,** average tube thickness. **e,** A confocal

reconstruction of the 3D network structure of the CD31 positive cells and **f,** the appearance of a central lumen within the network structures suggested they were hollow nascent vessels, e.g. tubular structures.

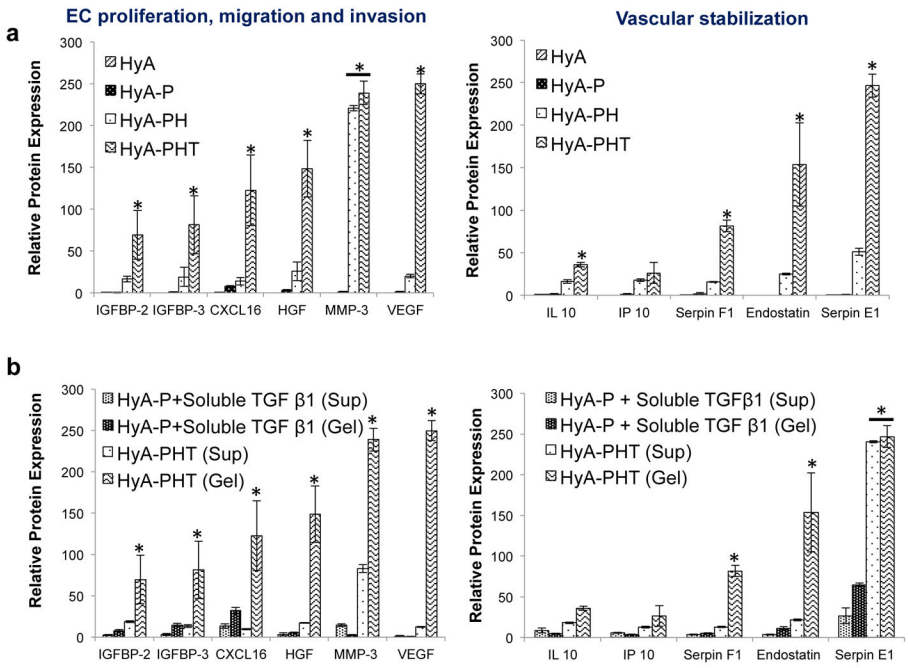

Figure 5. HyA-PHT hydrogels encouraged angiogenic cytokine expression by CPCs

a, The concentration of secreted angiogenic factors produced by CPCs and sequestered within HyA-PHT hydrogel after 12 days. To determine the secreted angiogenic factors, hydrogels were degraded by adding the 100 unit/mL of hyaluronidase at 37°C for 6 hr. Subsequently, degraded hydrogels were incubated with heparinase I, II & III at the 2.5 unit/mL concentration of each at 37°C for another 6hr to remove the adhered heparin with the sequestered proteins. These include factors that promote EC proliferation and **b,** those associated with vascular stability. **c & d,** The presentation of TGFβ1 affected the production of angiogenic proteins detected in the cell supernatant (**Sup**) or within the hydrogel (**Gel**). HyA-PHT hydrogels (850Pa, 380μM bsp-RGD(15), 0.03wt% heparin, and 40nM TGFβ1) demonstrated significant increases in expression of proteins associated with proliferation and vascular stability relative to identical hydrogels (HyA-P) with an equimolar concentration of soluble TGFβ1 in the media, but without heparin.

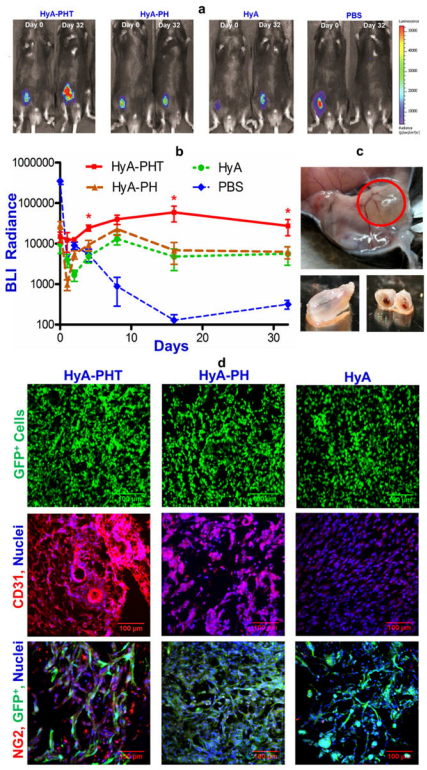

Figure 6. HyA-PHT hydrogels promoted CPC survival and endothelial differentiation *in vivo*

a, Bioluminescence post-implantation of GFP-fLuc-mCPCs (~500,000 cells in 100μL gel) in syngeneic mouse hindlimbs. **b**, Radiance generated by the transplanted CPCs over 32 days (n=5) demonstrated that the hydrogels promoted cell survival and limited cell diffusion away from the implantation site *in vivo*. **c**, The transplanted HyA-PHT hydrogels recruited host vessels to the exterior of the implant and a competent vasculature was evident throughout the cross section of the implants. **d**, Verification of the persistence of donor CPCs with GFP expression, and differentiation of CPCs into endothelial cells was confirmed by expression of CD31. HyA-PHT gels fostered significant and mature blood vessel formation, and infiltration of $NG2^+$ pericytes was observed with the donor GFP^+ cells. Scale bars = 100 μm.

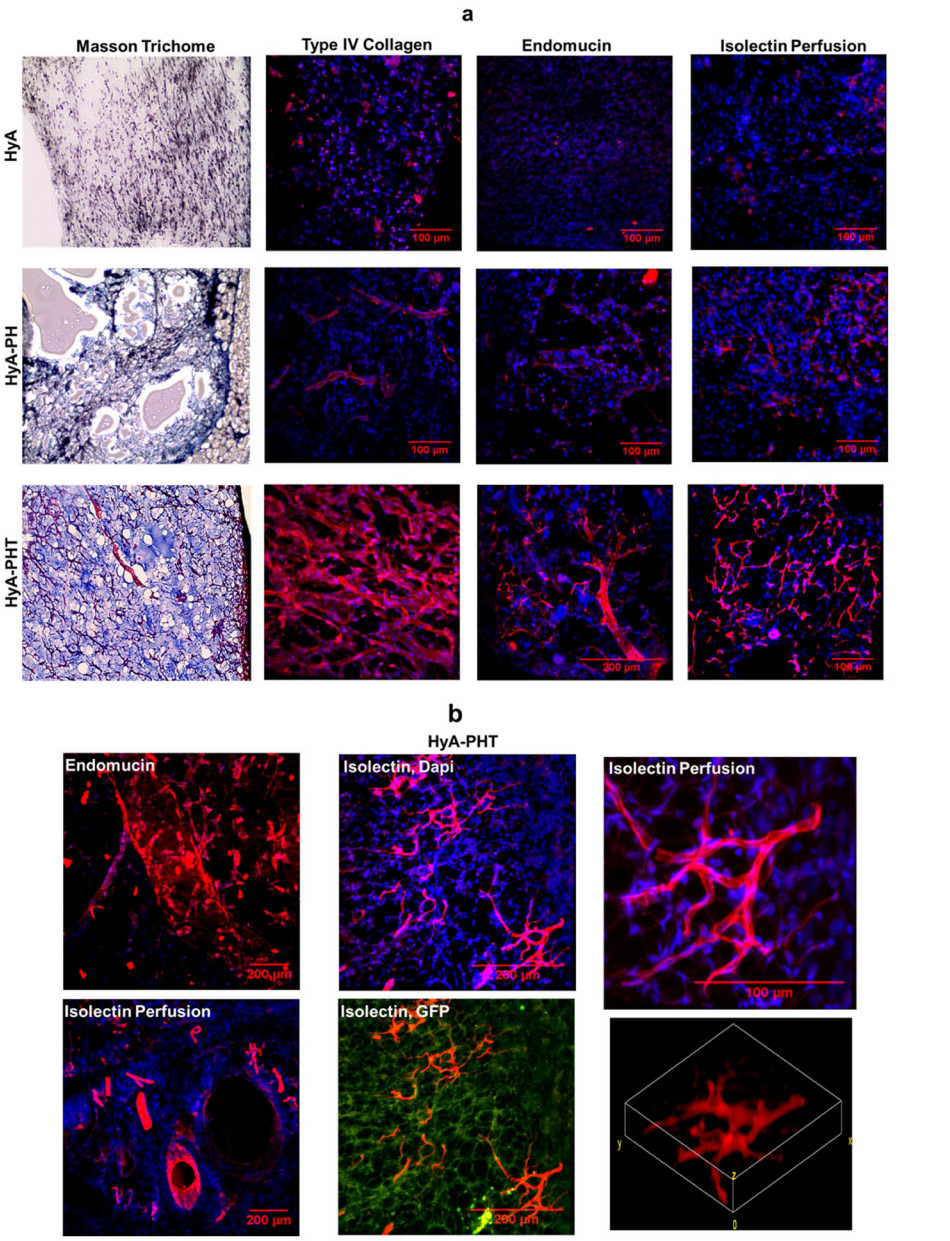

Figure 7. Extracellular matrix production and vascular tone assessed by histology

a, The HyA-PHT explants exhibited strong collagen staining by Massons's trichrome, which was rich with Type IV collagen, as visualized by immunohistochemistry. Vascular tone in the explants was evaluated by endomucin staining, and integration of the hydrogels with the host vasculature was assessed by systemic perfusion of the host with Alexa Fluor 568-conjugated GS-IB4 lectin (isolectin). **b,** Complex vascular structures were observed in the HyA-PHT explants by reconstruction of confocal images of endomucin staining and isolectin perfusion, the latter clearly indicating the vessels within the HyA-PHT hydrogel were anastomosed with the host vessels. Scale bars = 100 μm.